

ρ -meson properties at finite nuclear density*

L.A. Kondratyuk¹, A. Sibirtsev^{2†}, W. Cassing²
Ye.S. Golubeva³ and M. Effenberger²

¹ Institute of Theoretical and Experimental Physics,
117259 Moscow, Russia

² Institute for Theoretical Physics,
University of Giessen, D-35392 Giessen, Germany

³ Institute of Nuclear Research,
117312 Moscow, Russia

Abstract

We calculate the momentum dependence of the ρ -meson selfenergy based on the dispersion relation for the ρN scattering amplitude $f(\omega)$ at low nuclear density. The imaginary part of $f(\omega)$ is determined from the optical theorem, while the total ρN cross section is obtained within the VDM at high energy and within the resonance model at low energy. Our numerical results indicate a sizeable broadening of the ρ -meson width in the medium especially for low relative momenta p while the real part of the ρ selfenergy is found to change its sign and becomes repulsive already at momenta above 0.6 GeV/c. Extrapolating to nuclear saturation density ρ_0 we find a dropping of the ρ -mass for $p \approx 0$ in line with the QCD sumrule analysis of Hatsuda while at high energy an increase of the ρ -mass in line with the prediction by Eletsy and Joffe is obtained. However, when including a broadening of the baryonic resonances in the medium, the ρ -meson mass shift at $p \approx 0$ vanishes whereas the width increases substantially.

PACS: 25.20.-x; 25.20.Dc; 25.40Ep

Keywords: Photonuclear reactions; Photon absorption and scattering; vector mesons; meson-nucleon interactions

*Supported by DFG, Forschungszentrum Jülich and BMBF.

†On leave from the Institute of Theoretical and Experimental Physics, 117259 Moscow, Russia

1 Introduction

The properties of baryonic and mesonic resonances in the nuclear medium has received a vivid attention during the last years (cf. Refs. [1, 2, 3, 4, 5]) within the studies on the properties of hot and dense nuclear matter. Here, QCD inspired effective Lagrangian models [1, 4, 5] or approaches based on QCD sum rules [2, 3] predict that the masses of the vector mesons ρ and ω should decrease with the nuclear density. On the other hand, with a dropping hadron mass the phase space for its decay decreases, which results in a modification of its width or lifetime in matter, while due to interactions with the surrounding nuclear medium the resonance width will increase [6, 7, 8, 9].

The in-medium properties of vector mesons have been addressed experimentally so far by dilepton measurements at the SPS, both for proton-nucleus and nucleus-nucleus collisions [10, 11, 12, 13]. As proposed by Li *et al.* [14], the enhancement in $S + Au$ reactions compared to $p + Au$ collisions in the invariant mass range $0.3 \leq M \leq 0.7$ GeV might be due to a shift of the ρ meson mass. The microscopic transport studies in Refs. [15, 16, 17] for these systems point in the same direction, however, also more conventional selfenergy effects cannot be ruled out at the present stage [15, 18, 19, 20]. Especially the p-wave coupling of the ρ -meson to nucleons induces an attractive interaction at low relative momenta [20] which turns repulsive at large momenta. The explicit momentum dependence of the ρ -meson selfenergy thus is an important aspect to be investigated both, theoretically and experimentally e.g. by $\pi^- A$ reactions [8, 9, 21, 22].

The main goal of this paper is to calculate the explicit momentum dependence of the ρ -meson potential at finite nuclear densities within a dispersive approach that is based on the resonance model at low relative momenta of the ρ with respect to the nucleon at rest and the vector dominance model at high relative momenta following the suggestion by Eletsky and Joffe [23]. Our work is organized as follows: In Section 2 we briefly recall the relation between hadron self energies and the hadron-nucleon scattering amplitude at low density and discuss the dominant interaction mechanisms. In Section 3 we present our model for the γN scattering amplitude and the related dispersion relations. The ρN scattering amplitude then is evaluated in Section 4 within different models and their implications for the real and imaginary part of the ρ -meson selfenergy at finite nuclear density are presented in Section 5. A summary and discussion of open problems concludes this work in Section 6.

2 Hadronic resonances in the nuclear medium

The relativistic form of the wave equation describing the propagation of a mesonic resonance R in the nuclear matter is given as (see e.g. [9])

$$[-\nabla^2 + M_R^2 - iM_R\Gamma_R + U(\mathbf{r})] \Psi(\mathbf{r}) = E^2 \Psi(\mathbf{r}), \quad (1)$$

where $E^2 = \mathbf{p}^2 + M_R^2$ and \mathbf{p} , M_R and Γ_R are the momentum, mass and width of the resonance, respectively. The optical potential then is defined as

$$U(\mathbf{r}) = -4\pi f_{RN}(0) \rho_N(\mathbf{r}) \quad (2)$$

where $f_{RN}(0)$ is the forward RN -scattering amplitude and ρ_N is the nuclear density.

It is useful to rewrite Eq. (1) in the form

$$[\nabla^2 + \mathbf{p}^2] \Psi(\mathbf{r}) = [U(\mathbf{r}) - \Delta] \Psi(\mathbf{r}), \quad (3)$$

where

$$\Delta = P^2 - M_R^2 - iM_R\Gamma_R \quad (4)$$

is the inverse resonance propagator in the vacuum. The four-momentum P in Eq. (4) can be defined through the four-momenta of the resonance decay products, i.e.

$$P = p_1 + p_2 + \dots \quad (5)$$

When the resonance decays inside the nucleus of radius R_A at density ρ_N , the propagator has the form

$$\Delta^* = \Delta + 4\pi f(0)\rho_N = P^2 - M_R^{*2} + iM_R^*\Gamma_R^* \quad (6)$$

where

$$M_R^{*2} = M_R^2 - 4\pi \text{Re}f(0)\rho_N, \quad (7)$$

$$M_R^*\Gamma_R^* = M_R\Gamma_R + 4\pi \text{Im}f(0)\rho_N. \quad (8)$$

Its spectral function then can be described (in a first approximation) by a Breit–Wigner formula (nonrelativistically) as

$$F(M) = \frac{1}{2\pi} \frac{\Gamma_R^*}{(M - M_R^*)^2 + \Gamma_R^{*2}/4}, \quad (9)$$

which contains the effects of collisional broadening,

$$\Gamma_R^* = \Gamma_R + \delta\Gamma \quad (10)$$

with

$$\delta\Gamma = \gamma v \sigma_{RN} \rho_N, \quad (11)$$

and a shift of the meson mass

$$M_R^* = M_R + \delta M_R \quad (12)$$

with

$$\delta M_R = -\gamma v \sigma_{RN} \rho_N \alpha. \quad (13)$$

In Eqs. (11),(13) v is the average resonance velocity with respect to the target at rest, γ is the associated Lorentz factor, ρ_N is the nuclear density while σ_{RN} is the resonance-nucleon total cross section and $\alpha = \text{Re}f(0)/\text{Im}f(0)$.

As follows from Eqs. (11) and (13) the resonance mass shift and collisional broadening of its width in the nuclear medium depend on the resonance momentum p . For high momenta $p \gg M_R$ collisional broadening becomes very large and the resonance contribution can not be clearly separated from the background anymore. Thus medium effects can, in general, be detected only for low or moderate momenta.

The sign of the resonance mass shift depends on the sign of the real part of the forward RN scattering amplitude which again depends on the momentum of the resonance. For example, at low momenta ($p \approx 0$) various authors [1, 2, 3, 4] predict a decreasing mass of the vector mesons ρ , ω and ϕ with the nucleon density, whereas Eletsky and Ioffe have argued recently [23] that the ρ -meson should become heavier in nuclear matter at momenta of 2-7 GeV/c. If the ratio α is small - which is actually the case for the reactions considered because many reaction channels are open - the broadening of the resonance will be the main effect. As it was shown in Ref. [24] the account of this effect can also essentially influence the predictions of QCD sum rules [2, 3]. Therefore it is useful to perform independent calculations for the real part of the ρN forward scattering amplitude which can also be used at low energies.

Another important point is that Eqs. (11) and (13) for the collisional broadening and mass shift are valid only at low densities when the resonance-nucleon scattering amplitude inside the nucleus is the same as in the vacuum. The discussion of this point will be presented in Section 4.2 explicitly.

An alternative approach is to calculate the ρ -meson spectral function in the nuclear medium by considering its 2π decay mode and taking into account the rescattering of pions on nucleons (see Ref. [25]). However, to prevent double counting one should be cautious combining both contributions - the direct ρN interaction and the ρN interaction by a 2π intermediate state - in the ρ -meson spectral function. Assuming that the resonance is produced as a $q\bar{q}$ -system we can describe its time evolution in the rest frame by the Wigner-Weisskopf [26] formalism

$$|\rho(t)\rangle = e^{-imt} \{e^{-\Gamma_\rho t/2} |q\bar{q}\rangle + [1 - e^{-\Gamma_\rho t}]^{1/2} |\pi\pi\rangle\}. \quad (14)$$

Let us estimate the parameter

$$\epsilon = \frac{\Gamma_\rho t_f}{2} = \frac{\lambda_f M_\rho \Gamma_\rho}{2p} = \frac{\Gamma_\rho}{2(\Gamma_\rho + p\sigma\rho_A)}, \quad (15)$$

which defines the relative contribution of $|q\bar{q}\rangle$ and $|\pi\pi\rangle$ components, calculated at the time t_f in the resonance frame. During this time the resonance passes the distance λ_f in the laboratory system. At high momenta $p \gg M_R$ the parameter ϵ is evidently small. For $p \leq M_R$ it depends on the magnitude of σ . Within the framework of the resonance model used in Sect.4.2 we have $v\sigma \simeq 50$ mb at $p \leq M_R$. In this case $\epsilon \simeq 0.2$ and thus also small. Therefore we will take into account only the direct ρN interaction in our present study.

3 Photon-nucleon forward scattering amplitude

Within the framework of the Vector Dominance Model (VDM) the Compton scattering amplitude can be expressed through the ρN , ωN and ϕN scattering amplitudes as

$$T_{\gamma N}(s, t) = \frac{e^2}{4\gamma_\rho^2} \left[T_{\rho N}(s, t) + \frac{\gamma_\rho^2}{\gamma_\omega^2} T_{\omega N}(s, t) + \frac{\gamma_\rho^2}{\gamma_\phi^2} T_{\phi N}(s, t) \right]. \quad (16)$$

Here $T_{VN}(s, t)$ is the invariant amplitude for the elastic scattering of the transverse polarized vector meson on the nucleon, $e^2/4\pi$ is the fine-structure constant, $T_{\gamma N}(s, t)$ is the invariant Compton scattering amplitude and $\gamma_\rho^2/4\pi=0.55$ [27, 28, 29]. According to experimental data (cf. [30]) the last 2 terms on the r.h.s. of Eq. (16) can be neglected as compared to the first term. Then the ρN scattering amplitude can be expressed directly through the Compton amplitude.

The scattering amplitude $f(\omega, \theta)$, which enters into Eqs. (7),(8) for the resonance mass shift and collisional broadening can be expressed through the invariant scattering amplitude by

$$T(s, t) = 8 \pi \sqrt{s} \frac{p_{cm}}{p_{lab}} f(\omega, \theta), \quad (17)$$

where p_{cm} , p_{lab} are the momenta of the incident particle in the c.m. and laboratory systems, respectively, while θ is the scattering angle in the laboratory frame.

The real part of the forward γN scattering amplitude is related to the imaginary part through the dispersion relation (cf. Ref. [31])

$$Re f(\omega) = Re f(\omega_0) + \frac{2(\omega^2 - \omega_0^2)}{\pi} P \int_{\omega_{min}}^{+\infty} \frac{d\omega' \omega' Im f(\omega')}{(\omega'^2 - \omega_0^2)(\omega'^2 - \omega^2)}, \quad (18)$$

where $\omega = \omega_0$ is the subtraction point and ω_{min} is the threshold energy. The imaginary part of the forward scattering amplitude $Im f(\omega)$, furthermore, is related to the total cross section by the optical theorem,

$$Im f(\omega) = \frac{p_{lab}}{4\pi} \sigma_{tot}(\omega). \quad (19)$$

Thus the knowledge of the total cross section $\sigma_{tot}(\omega)$ is sufficient to determine $Re f(\omega)$ through the dispersion relation (18).

To obtain the real part of the Compton forward scattering amplitude one can perform the subtraction at $\omega_0 = 0$ turning (18) to the classical Kramers-Kronig relation [32, 33] with $\omega_{min} = m_\pi + m_\pi^2/2m_N$, $f_{\gamma p}(0) = -e^2/(4\pi m_N)$ and $f_{\gamma n}(0) = 0$. Here m_N and m_π are the masses of the nucleon and pion, respectively.

In the present approach the photoproduction cross section is calculated for $\omega < 1.5$ GeV within the resonance model by

$$\sigma_{\gamma p}^{tot}(s) = \sum_j \sigma_{\gamma p}^{R_j}(s) + \sigma_{\gamma p}^{BG}(s), \quad (20)$$

where the resonance contributions $\sigma_{\gamma p}^{R_j}(s)$ as well as the background term $\sigma_{\gamma p}^{BG}(s)$ were taken from Ref. [6]. At higher energies ($\omega \geq 1.5$ GeV), where the data do not have any resonance structure, we use the Regge parametrization from Donnachie and Landshoff [34].

In Fig. 1 we show our parametrization for the γp cross section in comparison with the available data [35]. The real part of the Compton scattering amplitude, calculated with the dispersion relation (18), is shown in Fig. 2. The agreement between our calculation and the experimental results for the real part of the Compton scattering amplitude [36] is quite satisfactory.

In Fig. 3 we compare our result with the data [35, 37] for the forward differential $\gamma p \rightarrow \gamma p$ cross section, which is given as

$$\left. \frac{d\sigma(\gamma p \rightarrow \gamma p)}{dt} \right|_{t=0} = \frac{\sigma_{tot}^2(\gamma p)}{4\pi} (1 + \alpha_{\gamma p}^2) \quad (21)$$

with $\alpha_{\gamma p} = \text{Re}f(\omega)/\text{Im}f(\omega)$. The solid line in Fig. 3 shows our calculation with Eq. (21) which is slightly below the experimental data in the Δ - resonance region. This disagreement is due to the neglect of the spin-flip term in Eq. (21). Indeed the spin structure of the Compton forward scattering amplitude has the following form [38],

$$\hat{f}(\omega) = \phi_f^* \left\{ f(\omega) \boldsymbol{\epsilon}_{fT}^* \cdot \boldsymbol{\epsilon}_{iT} + i\boldsymbol{\sigma} [\boldsymbol{\epsilon}_{fT}^* \times \boldsymbol{\epsilon}_{iT}] g(\omega) \right\} \phi_i, \quad (22)$$

where ϕ_i and ϕ_f are the Pauli spinors for the initial and final nucleons, while $\boldsymbol{\epsilon}_{iT}$ and $\boldsymbol{\epsilon}_{fT}$ are the transverse polarization vectors for the initial and final photons. In Eq. (22) $g(\omega)$ is the spin flip amplitude neglected in Eq. (21).

Actually, the former means that $\alpha_{\gamma p}^2$ in Eq. (21) should be substituted by the sum $\alpha_{\gamma p}^2 + \alpha_{s.f.}^2$ where $\alpha_{s.f.} = g(\omega)/f(\omega)$. For the γp scattering amplitude through the Δ -resonance we have $\alpha_{s.f.}(\Delta)=0.5$. Since the contribution from the Δ isobar is dominant at photon energies around 300 MeV, the relative contribution of the spin-flip term to the differential cross section in the Δ resonance region is about 20-25 % [30]. The dashed line in Fig. 3 is calculated when taking into account the spin-flip term near the Δ isobar. Indeed, the agreement with the data improves substantially.

We conclude, that the dispersion calculations for the real part of the forward $f_{\gamma p}$ scattering amplitude are quite reliable and consistent with the available experimental data.

4 The ρ -nucleon scattering amplitude in vacuum

4.1 ρN total cross section from photoproduction and Compton scattering

Within the VDM we can express the ρN scattering amplitude not only through the Compton scattering amplitude (Eq. (16)) but also through the amplitude for ρ - photoproduction:

$$T_{\rho N}(s, t) = \frac{2\gamma_\rho}{e} T_{\gamma N \rightarrow \rho N}(s, t). \quad (23)$$

Furthermore, the ρN total cross section can be related to the differential cross section of the reaction $\gamma p \rightarrow \rho p$ as

$$\sigma_{\rho p}^2 = \frac{\gamma_\rho^2}{4\pi} \frac{64\pi}{\alpha} \frac{1}{1 + \alpha_{\rho p}^2} \left(\frac{q_\gamma}{q_\rho} \right)^2 \left. \frac{d\sigma_{\gamma p \rightarrow \rho p}}{dt} \right|_{t=0}. \quad (24)$$

Here q_γ and q_ρ are the c.m. momenta of the γN and ρN systems at the same invariant collision energy \sqrt{s} . Moreover, we assume that the ratio $\alpha_{\rho p}$ of the real to imaginary part of the ρN forward scattering amplitude is small. This assumption is valid at least for energies above 3 GeV [30].

In Fig.4 we show the imaginary part of the ρN forward scattering amplitude calculated by Eq. (23) from the ρ photoproduction data [27, 28, 29] (dots) and with Eq. (16) from the Compton scattering data (solid line). We find a systematic disagreement between those two results at energies above 3-4 GeV. The main reason for this discrepancy is the 'blindness' of the photon coupling to other hadronic states except for the ρ -meson in Eqs. (16) and (23). Apart from the ω and ϕ contributions to the r.h.s. of Eq. (16) (which are relatively small), there might be more important contributions from the continuum spectrum of $X_{cont} = 2\pi, 3\pi, \text{etc.}$ final states. The amplitudes of these contributions describe diagonal transitions $XN \rightarrow XN$ which do not vanish at high energies as well as the $\rho N \rightarrow \rho N$ transition.

On the other hand relation (23) can only be violated because of nondiagonal transitions $XN \rightarrow \rho N$. The relative contribution of these transitions, except for a small diffractive part, vanishes at high energies. It is known that the diffractive cross section in the case of $\pi N \rightarrow XN$ reaction is about 20-25 % of the elastic πN scattering cross section at 5-30 GeV (see [39] and references therein). It seems reasonable to assume that similar results will be also valid for the ρN interaction. Therefore, we expect that the relation (16) should be less accurate as compared to relation (23) and we shall calculate the ρN total cross section in the following using Eq. (24).

4.2 The resonance model combined with VDM

If VDM would be valid at all energies we could calculate the mass shift and collisional broadening of the ρ meson in nuclear matter at low densities by inserting Eq. (16) or Eq. (23) in Eqs. (7) and (8) from Sect. 2. However, the VDM is expected to hold only at high energies $\omega > 2$ GeV [40]. At lower energies ($\omega \leq 1.5$ GeV) there are a lot of baryonic resonances which couple rather strongly to the transverse as well as to the longitudinal ρ -mesons [41]. Therefore at low energies it is better to describe the ρN interaction within the framework of resonance model [25, 42].

Experimental information on the baryonic resonances is only available for masses below $\simeq 2$ GeV. At higher energies we thus calculate the total cross section of the ρN interaction within the VDM using Eq. (24) or the Quark Model (QM), alternatively, where $\sigma_{\rho N}$ can be expressed in terms of pion-nucleon cross sections as

$$\sigma_{\rho^0 N} = \frac{1}{2} (\sigma_{\pi^- N} + \sigma_{\pi^+ N}), \quad (25)$$

and the πN cross sections can be taken from a Regge fit to the experimental data [34].

With proper parametrizations for the ρN total cross section at all energies we then can finally reconstruct the real part of the forward scattering amplitude by the dispersion relation (18). In the following we consider the ρN forward scattering amplitude being averaged over the ρ -meson transverse and longitudinal polarizations.

We saturate the ρN total cross section at low energies by the resonances listed in Table 1. For the Breit-Wigner contribution of each resonance we adopt the approach developed by Manley and Saleski [43]. In this model the total ρN cross section is given

as a function of the ρ -meson mass m and the invariant collision energy \sqrt{s} by:

$$\sigma_{\rho N}(m, \sqrt{s}) = \frac{2\pi}{3q_\rho^2} \sum_R (2J_R + 1) \frac{s\Gamma_{\rho N}^{in}(m, \sqrt{s})\Gamma_{tot}(\sqrt{s})}{(s - M_R^2)^2 + s\Gamma_{tot}^2(\sqrt{s})}, \quad (26)$$

where q_ρ denotes the c.m. momentum of the ρN system, J_R the spin of the resonance, M_R the pole mass and Γ_{tot} the total width as sum over the partial channels. For the case of an unstable particle in the final channel the partial width has to be integrated over the spectral function of this particle. The energy dependence of the partial width $\Gamma_{\rho N}$ for the decay of each baryonic resonance into the ρN channel, i.e. $R \rightarrow \rho N$, is given by

$$\Gamma_{\rho N}(\sqrt{s}) = \Gamma_{\rho N}(M_R) \frac{g(\sqrt{s})}{g(M_R)}, \quad (27)$$

where $\Gamma_{\rho N}(M_R)$ is the ρN partial width at the resonance pole M_R , while the function $g(\sqrt{s})$ is determined as

$$g(\sqrt{s}) = \int_{2m_\pi}^{\sqrt{s}-m_N} A_\rho(m') \frac{q_{\rho N}(m')}{\sqrt{s}} B_l^2(q_{\rho N}) dm'. \quad (28)$$

Here $q_{\rho N}(m')$ is the c.m. momentum of the nucleon and the ρ -meson with mass m' , B_l is a Blatt–Weisskopf barrier penetration factor, l denotes the angular momentum of the ρN system and A_ρ is the spectral function of the ρ -meson in free space taken as

$$A_\rho(m) = \frac{2}{\pi} \frac{m^2 \Gamma_\rho(m)}{(m^2 - M_\rho^2)^2 + m^2 \Gamma_\rho^2(m)}, \quad (29)$$

where $M_\rho=770$ MeV and the mass dependent width $\Gamma_\rho(m)$ of the ρ -meson is given by

$$\Gamma_\rho(m) = \frac{\Gamma_\rho^0 M_\rho}{m} \left[\frac{q_{\pi\pi}(m)}{q_{\pi\pi}(M_\rho)} \right]^3 \left[\frac{1 + \delta^2 q_{\pi\pi}^2(M_\rho)}{1 + \delta^2 q_{\pi\pi}^2(m)} \right]^2 \quad (30)$$

with $\delta = 5.3$ (GeV/c) $^{-1}$ and $\Gamma_\rho^0 = 150$ MeV.

The incoming width in Eq. (26) reads:

$$\Gamma_{\rho N}^{in}(m, \sqrt{s}) = C_{\rho N}^{I_R} \frac{q_{\rho N}(m)}{\sqrt{s}} B_l^2(q_{\rho N}) \frac{\Gamma_{\rho N}(M_R)}{g(M_R)}, \quad (31)$$

where $C_{\rho N}$ denotes the appropriate Clebsh-Gordan coefficient for the coupling of the isospins of ρ and nucleon to the isospin I_R of the resonance. The properties of the baryonic resonances coupled to the ρ are listed in Table 1; in the following calculations we exclude the resonances with one star confidence level.

Within the resonance model we can evaluate the total ρN cross section as the function of two variables: the ρ momentum and the invariant mass m of the ρ -meson. Fig. 5 shows the momentum dependence of the total ρN cross section for different masses of the ρ -meson, respectively. At higher momenta ($p_\rho \geq 1.5$ GeV/c), where the total cross section is described by VDM or the QM, we assume that it does not depend on m .

In Fig. 6 the solid line represents the prediction of the resonance model for the total ρN cross section averaged over the ρ -meson spectral function A_ρ while the result from the quark-model (QM) is shown by the dashed line. The solid circles in Fig. 6 show the total ρp cross section obtained by Eq. (24) and the experimental forward ρ -photoproduction data from [27, 28, 29]. Furthermore, the squares in Fig. 6 show the ρN cross section extracted from the reaction $\gamma + d \rightarrow \rho^0 + d$ independently of the VDM [44]. The results for the total cross section of the ρN interaction calculated within the framework of the quark-model (QM) and the VDM are in fair agreement at momenta above 2 GeV/c. The dotted line in Fig. 6 shows the interpolation between the low and high energy parts of the total ρp cross section which we will adopt furtheron.

To compute the real part of the amplitude we use the dispersion relation (18) and perform the subtraction at $\omega_0 = 4.46$ GeV. Moreover, $Ref(\omega_0)$ at the subtraction point was calculated with the VDM from the ρ -meson photoproduction differential cross section measured by DESY-MIT [45] and the Daresbury group [46]. Since the resonance model is also valid below the ρN threshold, the ρ contribution in this case is calculated as an integral over the available invariant mass of the 2π system.

The real and imaginary parts of the $f_{\rho N}$ amplitude - calculated with the total ρN cross section averaged over the ρ -meson spectral function in free space (29) - are shown in Fig. 7. The imaginary part corresponds to the total ρp cross section from Fig. 6 using the dashed line as an interpolation. The real part of the $f_{\rho N}$ amplitude is in line with the rescaled real part of the Compton forward scattering amplitude only for momenta $p_\rho \simeq 6$ GeV/c, where both are negative. However, with decreasing ρ -meson momentum the real part $Ref_{\rho N}$ changes the sign at $p_\rho \approx 0.6$ GeV/c.

This behaviour of the real part for the $f_{\rho N}$ amplitude has its origin in the resonance contribution at low energies. To illustrate this argument we present in Fig. 8 $Ref_{\rho N}$ neglecting the part of the ρN cross section from the resonance model. We find that in this case the real part does not change its sign and remains negative over the whole momentum range.

Furthermore, Fig. 9 shows the real part of the forward ρN scattering amplitude calculated for the different masses of the two pion system m coupled to the ρ -meson. We find that $Ref_{\rho N}$ substantially depends on the ρ -meson mass. Note that the dip for $p_\rho \simeq 1$ GeV/c is due to our interpolation between the low and the high energy regions and thus an artefact of our model which should be discarded. We also have to mention that the magnitude of the ρ -meson momentum, where the real part of the forward ρN scattering amplitude changes its sign, depends on the prescription for the transition between the resonance and high energy part of the total cross section, which is actually model dependent, and estimate this uncertainty as $\delta p_\rho = \pm 100$ MeV/c.

5 Mass shift and broadening of the ρ -meson in the nuclear medium

In the low density approximation one now can express the correction of the ρ -meson mass and width at finite nuclear density ρ_N through $f_{\rho N}$ using Eqs. (7) and (8).

We show the corresponding results for the mass and width of the ρ -meson in Fig. 10

calculated at saturation density $\rho_0 \approx 0.16 \text{ fm}^{-3}$ and with the averaged ρN cross section from the resonance model, as described above. The upper part of Fig. 10 also shows the most recent result from Hatsuda [52] calculated within the QCD sumrule approach at $\omega = m_\rho$ by the full dot. Our result for δm in the low density approximation is in agreement with this calculation for $p_\rho \approx 0$.

At high momenta $p \geq 2 \text{ GeV}/c$ our result is also in qualitative agreement with the VDM predictions for the mass shift as found by Eletsky and Ioffe [23]. Some discrepancy with the results from [23] might be caused by our i) different treatment of the low energy region and ii) by the use of the ρ photoproduction data for the reconstruction of the ρN total cross section and the experimental data for the real part of the ρN forward scattering amplitude at the subtraction point.

Therefore, if the low density approximation could be extrapolated up to ρ_0 , our model would demonstrate that the repulsive interaction of the ρ -meson at high momenta might be consistent with the attractive interaction at low energies. However, as it was shown recently in Ref. [24], the effect of the finite ρ width can essentially influence the predictions of QCD sum rules [2, 3]. Moreover, recent microscopic calculations of the ρ -spectral function at low energies do not show any substantial attraction for slow ρ -mesons at normal nuclear density [47].

Thus it is important to check if the results obtained within the low density approximation are still valid at normal nuclear density ρ_0 . In calculating the mass shift and broadening of the width for the ρ -meson (as shown in Fig. 10) we used the vacuum ρN scattering amplitude containing resonance contributions which, however, might be different in nuclear matter.

An indication for a possible strong medium-modification of baryonic resonances is the experimental observation that the total photoabsorption cross section in nuclei for $A \geq 12$ does not show any resonant structure except the $\Delta(1232)$ isobar [48, 49, 50]. As was shown in Ref. [6, 51] this might be explained by a strong in-medium broadening of the $D_{13}(1520)$ resonance ($\Gamma_{med} \simeq 300 \text{ MeV}$ compared to the vacuum width $\Gamma_R \simeq 120 \text{ MeV}$), but not by conventional medium effects like Fermi motion or Pauli blocking. While a collision broadening of this order is hard to justify, it might arise from the strong coupling of the D_{13} resonance to the ρN channel and a medium modification of the ρ -meson [42]. In Ref. [47] it has been shown that such a mechanism can lead to an in-medium width of the $D_{13}(1520)$ resonance of about 350 MeV.

To estimate how this effect influences our results we have performed also calculations for the in-medium ρN total cross section by assuming that at normal nuclear density the widths of all resonances - coupled to the ρN channel - are twice as in the vacuum, but their ρN branching ratios stay the same. This in-medium ρN cross section then was used in the dispersion relation for the calculation of the in-medium real part of the ρN forward scattering amplitude.

The results of these calculations are shown in Fig. 11 for the total pp cross section and the real part of the forward scattering amplitude calculated with different widths of all baryonic resonances. The factor κ in Fig. 11 stands for the ratio of the in-medium width of the baryonic resonance to its value in free space. We see that the medium effects have a strong influence on the ρN scattering amplitude in the resonance region. The total cross section becomes smoother in the low energy region and as a result the

real part of $f_{\rho N}(0)$ does not change sign anymore with decreasing p_ρ . At small p_ρ it remains negative and small, which means that the main medium effect for the ρ -meson at normal nuclear density is the collisional broadening; the mass shift is almost absent. This result is in qualitative agreement with recent calculations of the ρ -meson spectral function at low energies [5, 18, 47].

6 Conclusions

In summary, we have calculated the momentum dependence of the ρ -meson selfenergy (or in-medium properties) based on the dispersion relation (18) for the ρN scattering amplitude at finite nuclear density. The imaginary part of $f(\omega)$ is calculated via the optical theorem (19) while the total ρN cross section is obtained within the VDM at high energy and within the resonance model at low energy. Our numerical results indicate a sizeable broadening of the ρ -meson width in the medium especially for low relative momenta p_ρ . In the low density approximation the real part of its selfenergy is found to be attractive for $p_\rho \leq m_\rho$ and to change its sign, becoming repulsive at higher momenta in line with the prediction by Eletsky and Joffe [23]. Extrapolating the low density approximation to nuclear saturation density we obtain a dropping of the ρ -mass at $p_\rho \approx 0$ in line with the QCD sumrule analysis of Hatsuda [52]. However, the resonance part of the ρN scattering amplitude is also influenced by the nuclear medium at saturation density so much that the moderate attraction at $p_\rho \simeq 0$ changes to a comparatively small repulsion. This behaviour of the ρ -meson selfenergy is in qualitative agreement with the recent microscopic calculations of Rapp, Chanfray and Wambach [18] as well as Klingl et al. [5] for the ρ spectral function.

We note that the explicit momentum dependence of the ρ -meson selfenergy is an important issue that has to be incorporated e.g. in transport theories that attempt to extract information on the ρ spectral function in comparison to experimental dilepton data.

The authors acknowledge many helpful discussions with K. Boreskov, E.L. Bratkovskaya, V.L. Eletsky, B.L. Ioffe, S. Leupold, U. Mosel and Yu. Simonov throughout this study.

References

- [1] G. Brown and M. Rho, Phys. Rev. Lett. **66**, 2720 (1991).
- [2] T. Hatsuda and S. Lee, Phys. Rev. C **46**, R34 (1992).
- [3] M. Asakawa and C.M. Ko, Phys. Rev. C **48**, R526 (1993).
- [4] C.M. Shakin and W.-D. Sun, Phys. Rev. C **49**, 1185 (1994).
- [5] F. Klingl and W. Weise, Nucl. Phys. **A606**, 329 (1996); F. Klingl, N. Kaiser, and W. Weise, Nucl. Phys. **A617**, 449 (1997); *ibid.* **A624**, 927 (1997) .

- [6] L. A. Kondratyuk, M. Krivoruchenko, N. Bianchi, E. De Sanctis, and V. Muccifora, Nucl. Phys. **A579**, 453 (1994).
- [7] K.G. Boreskov, J. Koch, L.A. Kondratyuk, and M.I. Krivoruchenko, Phys. of Atomic Nuclei **59**, 1908 (1996); K.G. Boreskov, L.A. Kondratyuk, M.I. Krivoruchenko, and J. Koch Nucl. Phys. **A619**, 295 (1997).
- [8] W. Cassing, Ye.S. Golubeva, A.S. Iljinov, and L.A. Kondratyuk, Phys. Lett. B **396**, 26 (1997).
- [9] Ye.S. Golubeva, L.A. Kondratyuk, and W. Cassing, Nucl. Phys. **A625**, 832 (1997).
- [10] G. Agakichiev et al., Phys. Rev. Lett. **75**, 1272 (1995).
- [11] M.A. Mazzoni, Nucl. Phys. **A566**, 95c (1994).
- [12] T. Åkesson et al., Z. Phys. C **68**, 47 (1995).
- [13] A. Drees, Nucl. Phys. **A610**, 536c (1996).
- [14] G.Q. Li, C.M. Ko, and G.E. Brown, Phys. Rev. Lett. **75**, 4007 (1995).
- [15] W. Cassing, W. Ehehalt, and C.M. Ko, Phys. Lett. B **363**, 35 (1995).
- [16] W. Cassing, W. Ehehalt, and I. Kralik, Phys. Lett. B **377**, 5 (1996).
- [17] E. L. Bratkovskaya and W. Cassing, Nucl. Phys. **A619**, 413 (1997).
- [18] R. Rapp, G. Chanfray, and J. Wambach, Phys. Rev. Lett. **76**, 368 (1996).
- [19] R. Rapp, G. Chanfray, and J. Wambach, Nucl. Phys. **A617**, 472 (1997).
- [20] B. Friman and H.J. Pirner, Nucl. Phys. **A617**, 496 (1997).
- [21] W. Schön, H. Bokemeyer, W. Koenig, and V. Metag, Acta Physica Polonica B **27**, 2959 (1996).
- [22] Th. Weidmann, E.L. Bratkovskaya, W. Cassing, and U. Mosel, nucl-th/971104.
- [23] V.L. Eletsky and B.L. Ioffe, Phys. Rev. Lett. **78**, 1010 (1997).
- [24] S. Leupold, W. Peters, and U. Mosel, nucl-th/9708016, Nucl. Phys. **A**, in press.
- [25] A. Sibirtsev and W. Cassing, nucl-th/9712009, Nucl. Phys. **A**, in press.
- [26] V. Weisskopf and E. Wigner, Z. Phys. **63**, 54 (1930).
- [27] R. Anderson, D. Gustavson, J. Johnson, D. Ritson, B.H. Wiik, W.G. Jones, D. Kreinick, F. Murphy, and R. Weinstein, Phys. Rev. D **1**, 27 (1970).
- [28] J. Ballam et al., Phys. Rev. D **7**, 3150 (1973).
- [29] R.M. Egloff et al., Phys. Rev. Lett. **43**, 657 (1979).

- [30] T.H. Bauer, R.D. Spital, D.R. Yennie, and F.M. Pipkin, *Rev. Mod. Phys.* **50**, 261 (1978).
- [31] J.D. Bjorken and S.D. Drell, *Relativistic Quantum Fields*, McGraw-Hill (1965) 209.
- [32] R. Krönig, *J. Op. Soc. Am.*, **12**, 547 (1926).
- [33] H.A. Kramers, *Atti Congr. Inter. Fisici Como* (1927).
- [34] A. Donnachie and P.V. Landshoff., *Phys. Lett. B* **296**, 227 (1992).
- [35] Landolt-Börnstein, New Series, ed. H. Schopper, I/12 (1988)
- [36] W. Pfeil, H. Rollnik, and S. Stankowski, *Nucl. Phys.* **A73**, 166 (1974).
- [37] H. Genzel, M. Jung, R. Wedemeyer, and H.J. Weyer, *Z. Phys. A* **279**, 399 (1976).
- [38] M. Damashek and F.J. Gilman, *Phys. Rev. D* **1**, 1319 (1970).
- [39] A.B. Kaidalov, *Phys. Rep.* **50**, 157 (1979).
- [40] B.L. Ioffe, V.A. Khoze, and L.N. Lipatov, *Hard Processes* (North-Holland, Amsterdam, 1984) Vol. 1.
- [41] Particle Data Group, *Phys. Rev. D* **54**, 1 (1996).
- [42] M. Effenberger, A. Hombach, S. Teis, and U. Mosel, *Nucl. Phys.* **A613**, 353 (1997); **A614**, 501 (1997).
- [43] D.M. Manley and E.M. Saleski, *Phys. Rev. D* **45**, 4002 (1992).
- [44] R.L. Anderson, D. Gustavson, J. Johnson, I. Overman, D.M. Ritson, and B.H. Wiik, *Phys. Rev. D* **4**, 3245 (1971).
- [45] H. Alvensleben et al., *Phys. Rev. Lett.* **25**, 1377 (1970); *Phys. Rev. Lett.* **27**, 444 (1971).
- [46] P.J. Biggs, D.W. Braben, R.W. Clift, E. Gabathuler, and R.E. Rand, *Phys. Rev. Lett.* **27**, 1157 (1971).
- [47] W. Peters, M. Post, H. Lenske, S. Leupold, and U. Mosel, nucl-th/9708004, *Nucl. Phys. A*, in press.
- [48] N. Bianchi et al., *Phys. Lett. B* **299**, 219 (1993); *Phys. Lett. B* **309**, 5 (1993); *Phys. Lett. B* **325**, 333 (1994); M. Anghinolfi et al., *Phys. Rev. C* **47**, R922 (1993).
- [49] N. Bianchi et al., *Phys. Rev. C* **54**, 1688 (1996).
- [50] Th. Frommhold, F. Steiper, W. Henkel, U. Kneissl, J. Ahrens, R. Beck, J. Peise, and M. Schmitz, *Phys. Lett. B* **295**, 28 (1992).

- [51] S. Boffi, Y. Golubeva, L.A. Kondratyuk, M.I. Krivoruchenko, and E. Perazzi, Phys. Atom. Nucl. **60**, 1193 (1997).
- [52] T. Hatsuda, nucl-th/9702002.

Table 1: Properties of baryonic resonances coupled to the ρ -meson; l denotes the angular momentum of the ρ meson while stars indicate the confidence level. In our calculations we discard resonances with one star C.L.

Resonance	J_R	M_R (MeV)	Γ_R (MeV)	l	$\rightarrow N\rho$ (%)	C.L.
$S_{11}(1650)$	1/2	1659	173	0	3	* * *
$S_{11}(2090)$	1/2	1928	414	0	49	*
$D_{13}(1520)$	3/2	1524	124	0	21	* * *
$D_{13}(1700)$	3/2	1737	249	0	13	* * *
$D_{13}(2080)$	3/2	1804	447	0	26	**
$G_{17}(2190)$	7/2	2127	547	2	29	* * *
$P_{11}(1710)$	1/2	1717	478	1	3	* * *
$P_{11}(2100)$	1/2	1885	113	1	27	*
$P_{13}(1720)$	3/2	1717	383	1	87	* * *
P_{13}	3/2	1879	498	1	44	
$F_{15}(1680)$	5/2	1684	139	1	5	* * *
$F_{15}(1680)$	5/2	1684	139	3	2	* * *
$F_{15}(2000)$	5/2	1903	494	1	60	**
$F_{15}(2000)$	5/2	1903	494	3	15	**
$S_{31}(1620)$	1/2	1672	154	0	29	* * *
$S_{31}(1900)$	1/2	1920	263	0	38	* * *
$D_{33}(1700)$	3/2	1762	599	0	8	* * *
$D_{33}(1940)$	3/2	2057	460	0	35	*
$P_{31}(1910)$	1/2	1882	239	1	10	* * *
$F_{35}(1905)$	5/2	1881	327	1	86	* * *
F_{35}	5/2	1752	251	1	22	

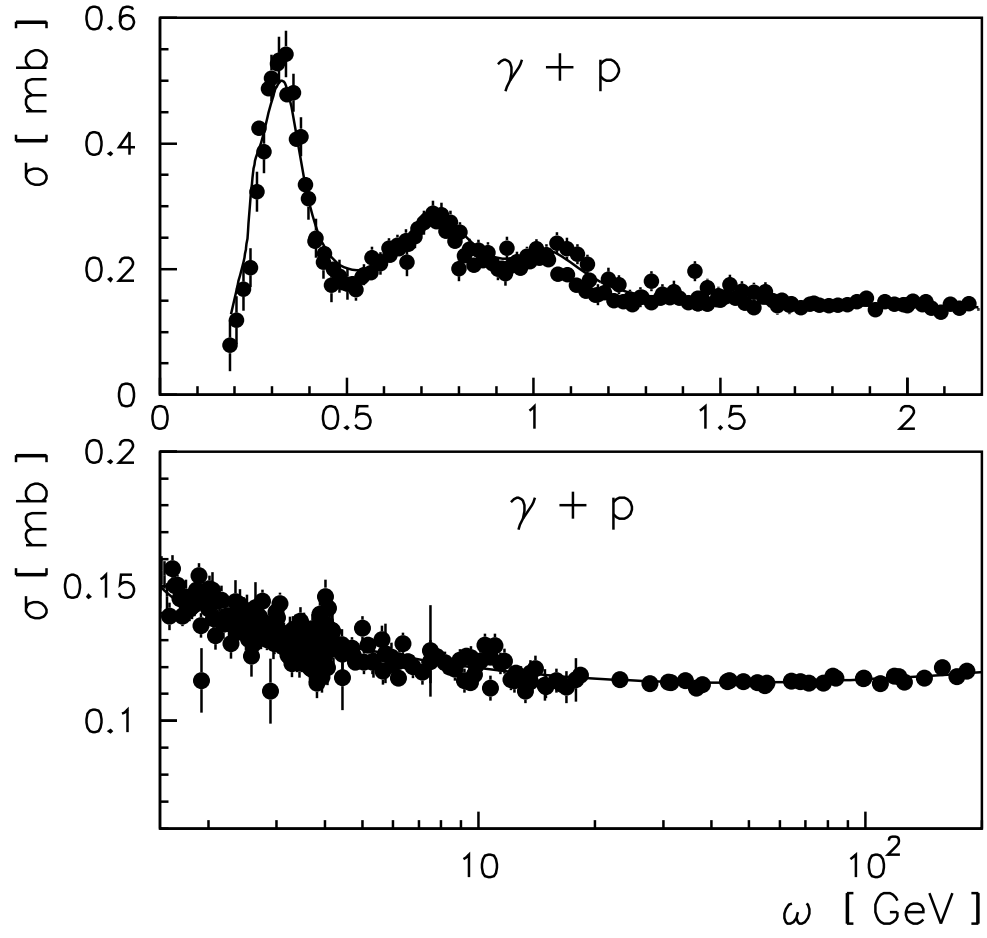


Figure 1: Cross section for γp interactions for $\omega \leq 2$ GeV and $\omega \geq 2$ GeV. The solid lines show our parametrization while the experimental data are taken from Ref. [35].

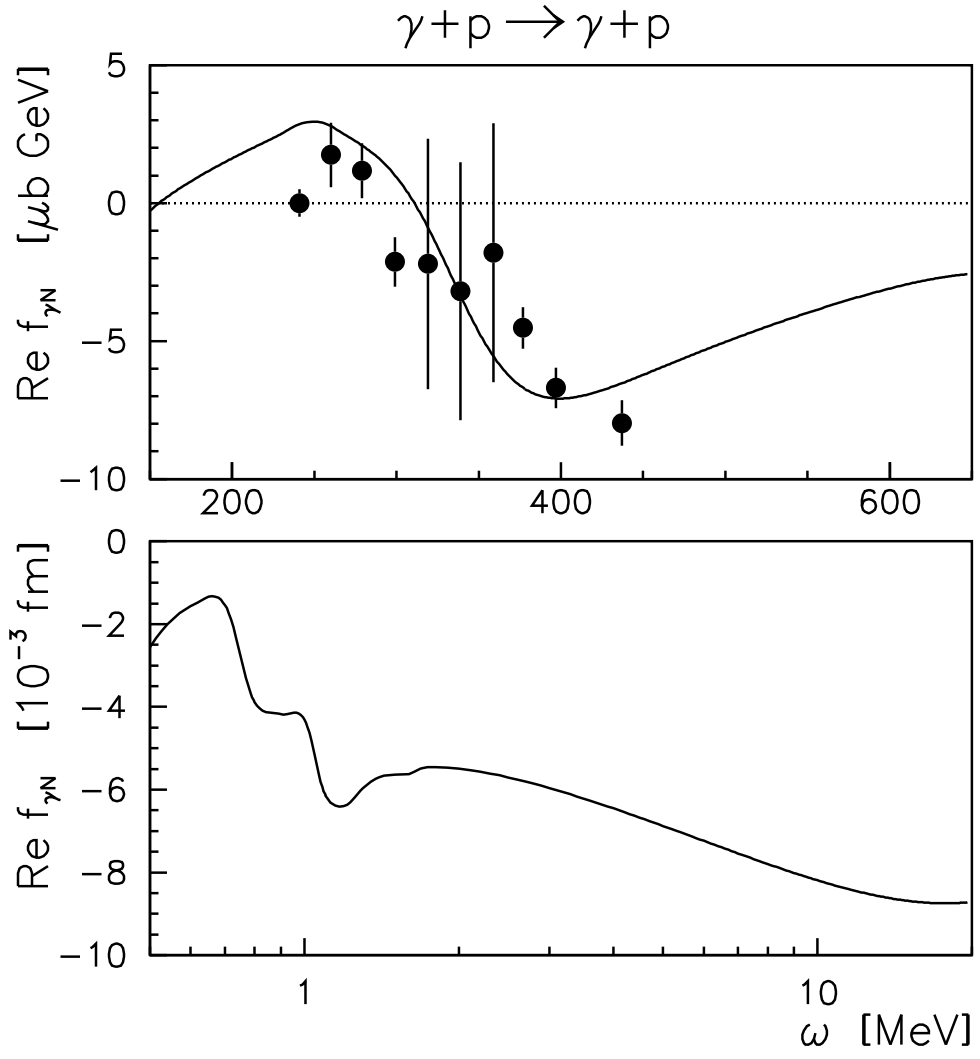


Figure 2: Real part of the Compton forward scattering amplitude. The solid lines show our calculations with the dispersion relation while the experimental data are taken from Ref. [36].

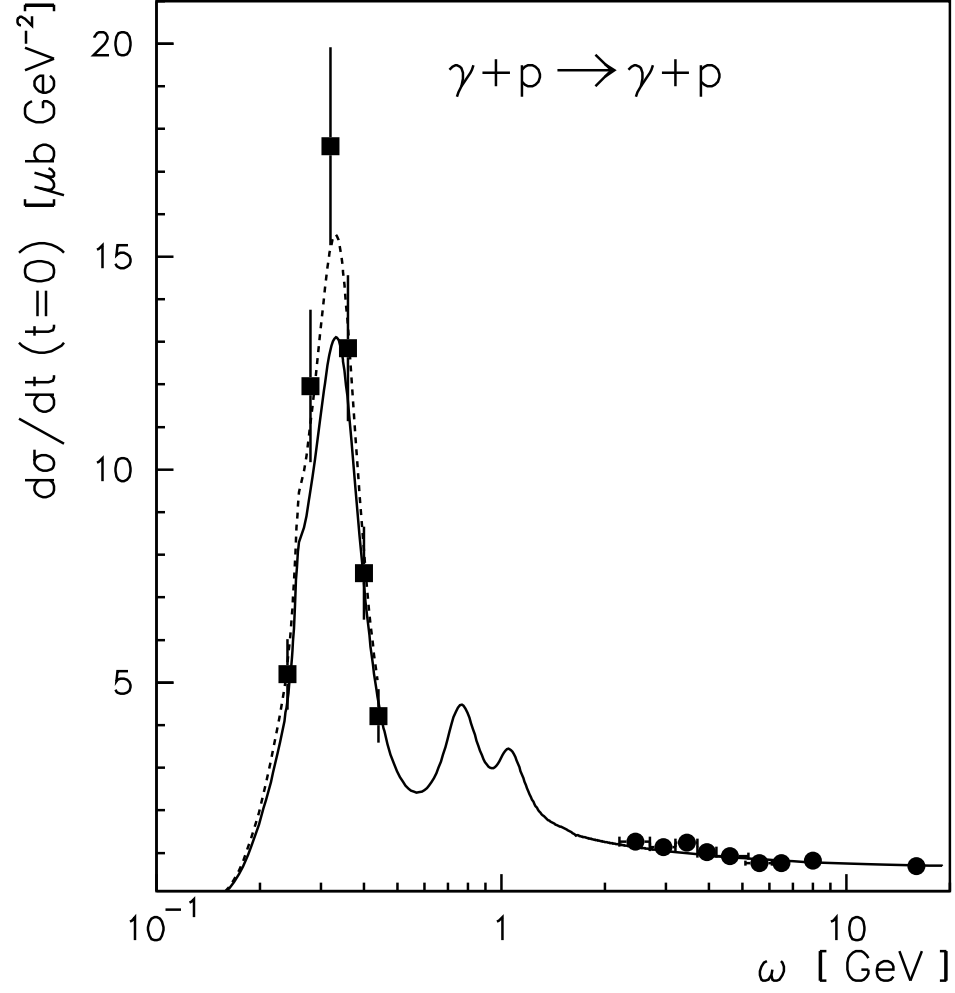


Figure 3: Differential cross section for Compton scattering at forward angle. The solid circles show the experimental data collected in Ref. [35] while the solid squares were taken from [37]. The lines are our calculation without (solid) and with inclusion of the spin-flip amplitude (dashed).

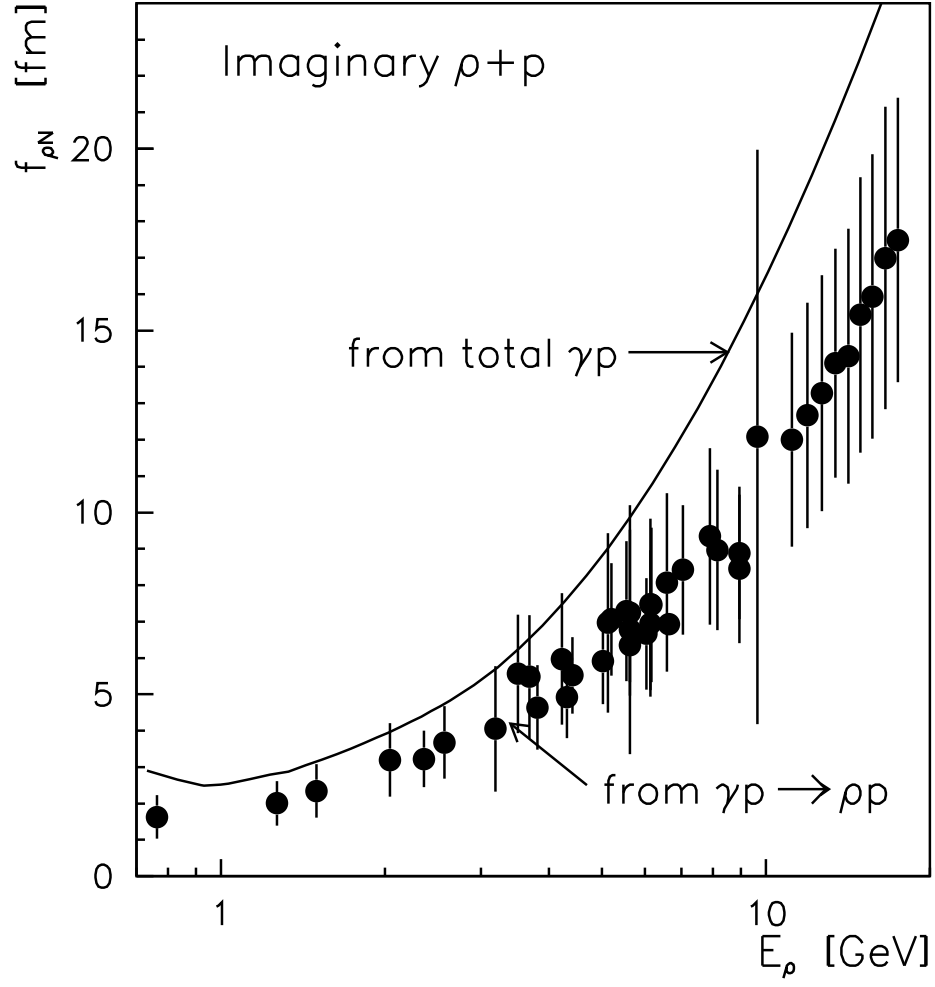


Figure 4: The imaginary part of the ρN forward scattering amplitude calculated from ρ -meson photoproduction [27, 28, 29] (dots) and from Compton scattering (solid line).

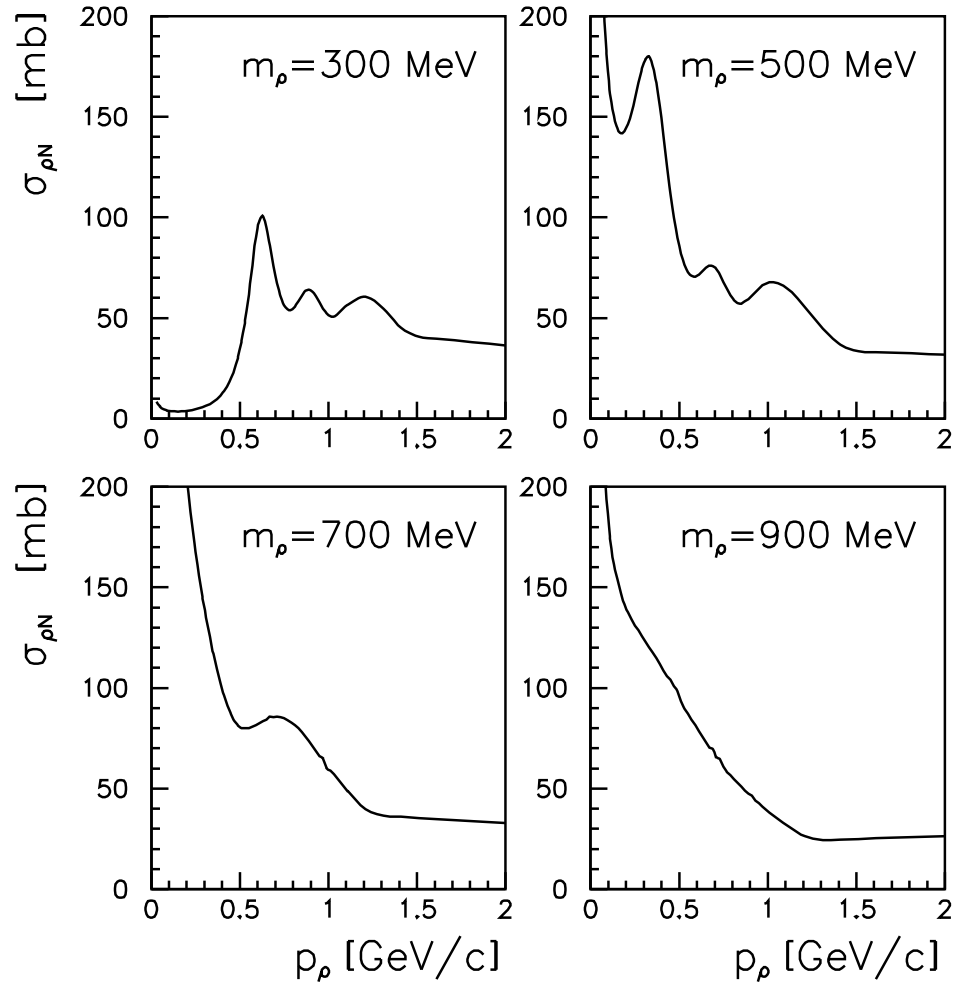


Figure 5: The total ρN cross section for different invariant masses of the ρ -meson. At low energy the cross section was obtained within the resonance model while at high energies it was extrapolated from the quark model (QM).

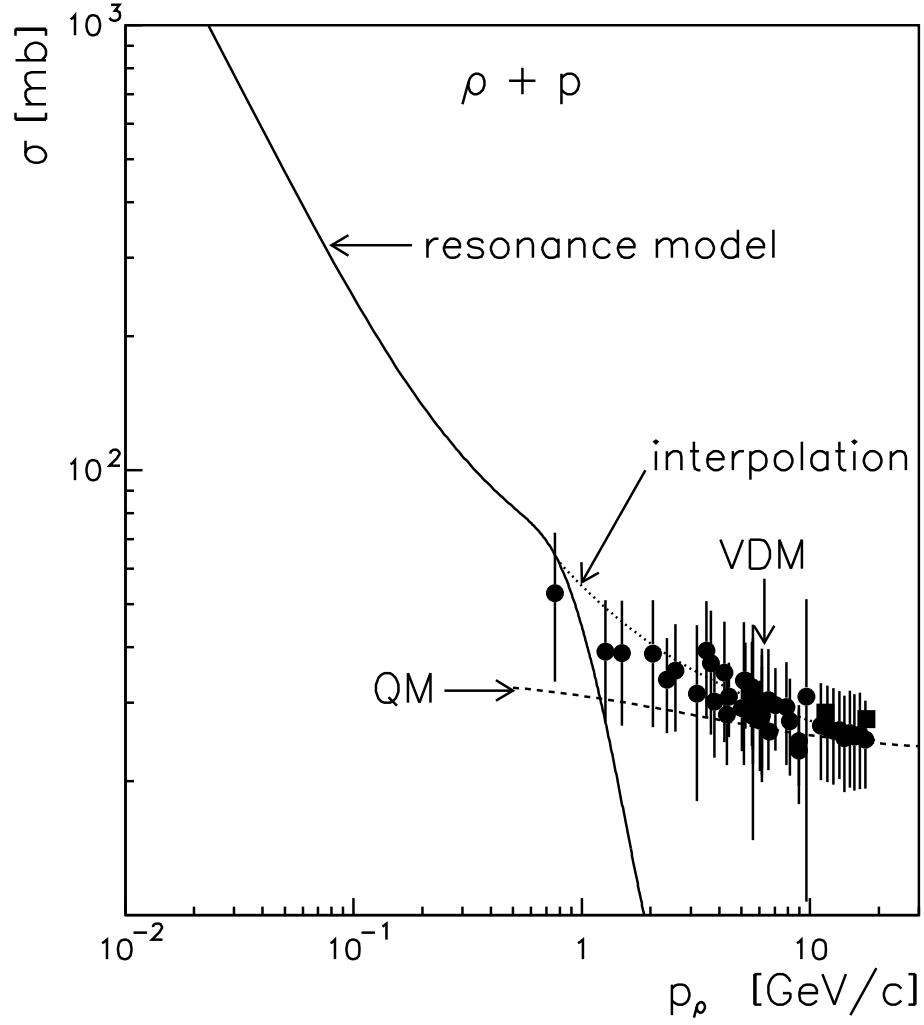


Figure 6: The total ρp cross section. The solid line shows our calculation within the resonance model while the dashed line is the result from the quark model (QM). The full circles show the experimental data extracted from ρ -photoproduction while the squares are from [44]. The dotted line indicates the interpolation that will be used furtheron.

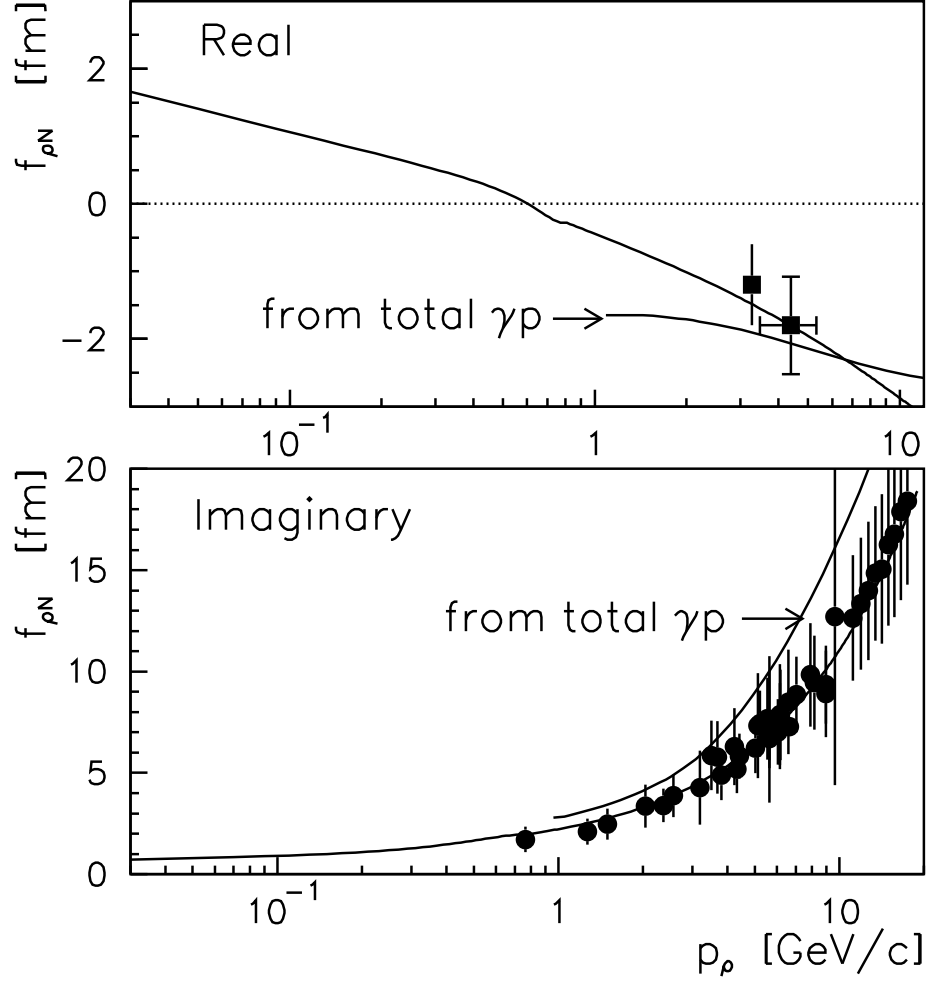


Figure 7: Real and imaginary part of the ρN scattering amplitude in free space. Our results calculated with the total ρN cross section are compared with the Compton scattering amplitude rescaled through VDM. The circles and squares are the results evaluated from the experimental data for ρ -meson photoproduction.

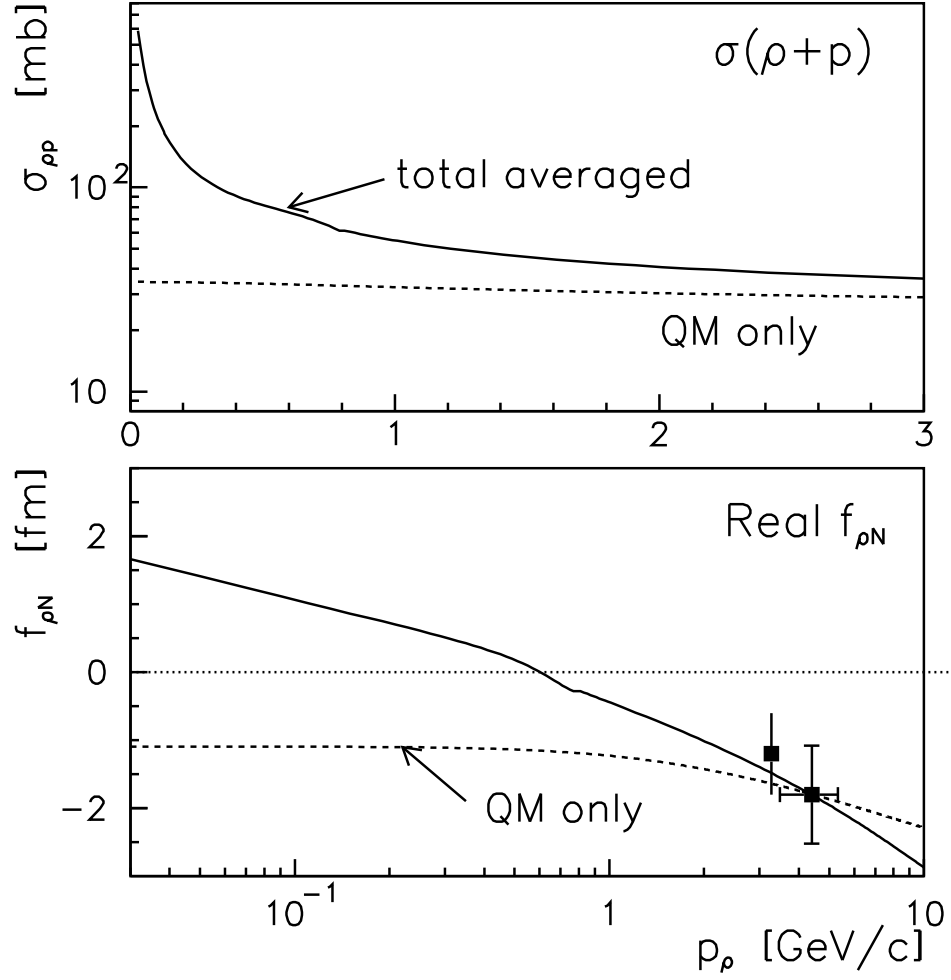


Figure 8: The total ρp cross section and the real part of the ρN scattering amplitude in free space as a function of the momentum p_ρ . The solid lines show our calculations with the total ρN cross section while the dashed lines indicate the results with the cross section from the quark model only. The squares are evaluated from the experimental data for ρ -meson photoproduction.

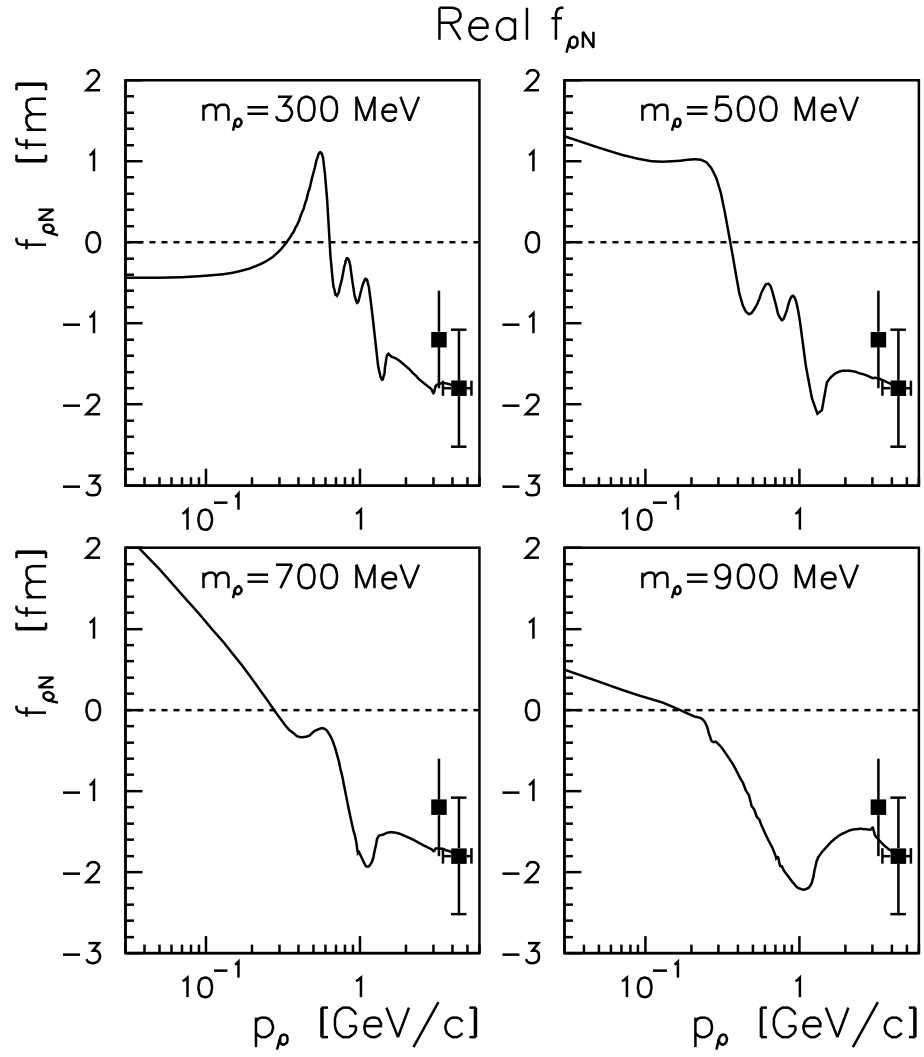


Figure 9: The real part of the ρN scattering amplitude in free space calculated for different masses of the ρ -meson. The squares are evaluated from the experimental data for ρ -meson photoproduction.

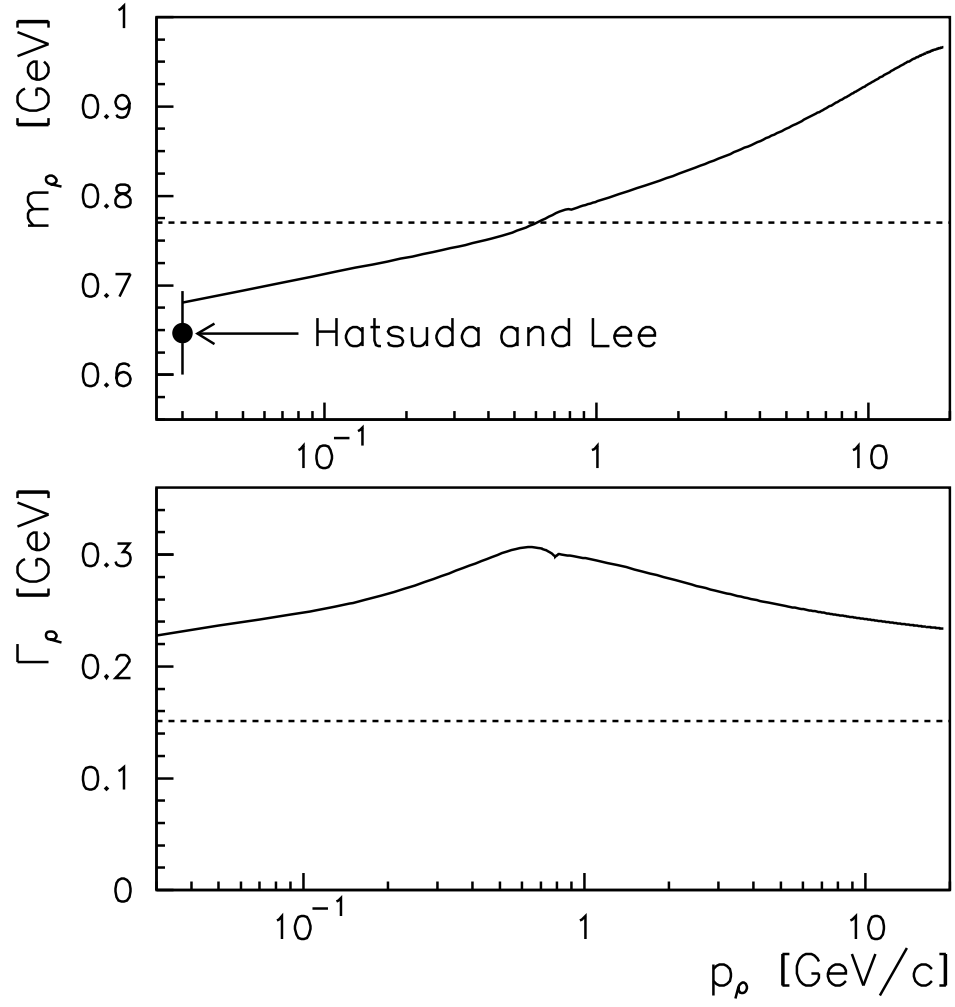


Figure 10: Mass and width of the ρ -meson at $\rho_N = 0.16 \text{ fm}^{-3}$ according to our model in the low density approximation. The full dot corresponds to the result from Hatsuda [52] within the QCD sumrule approach.

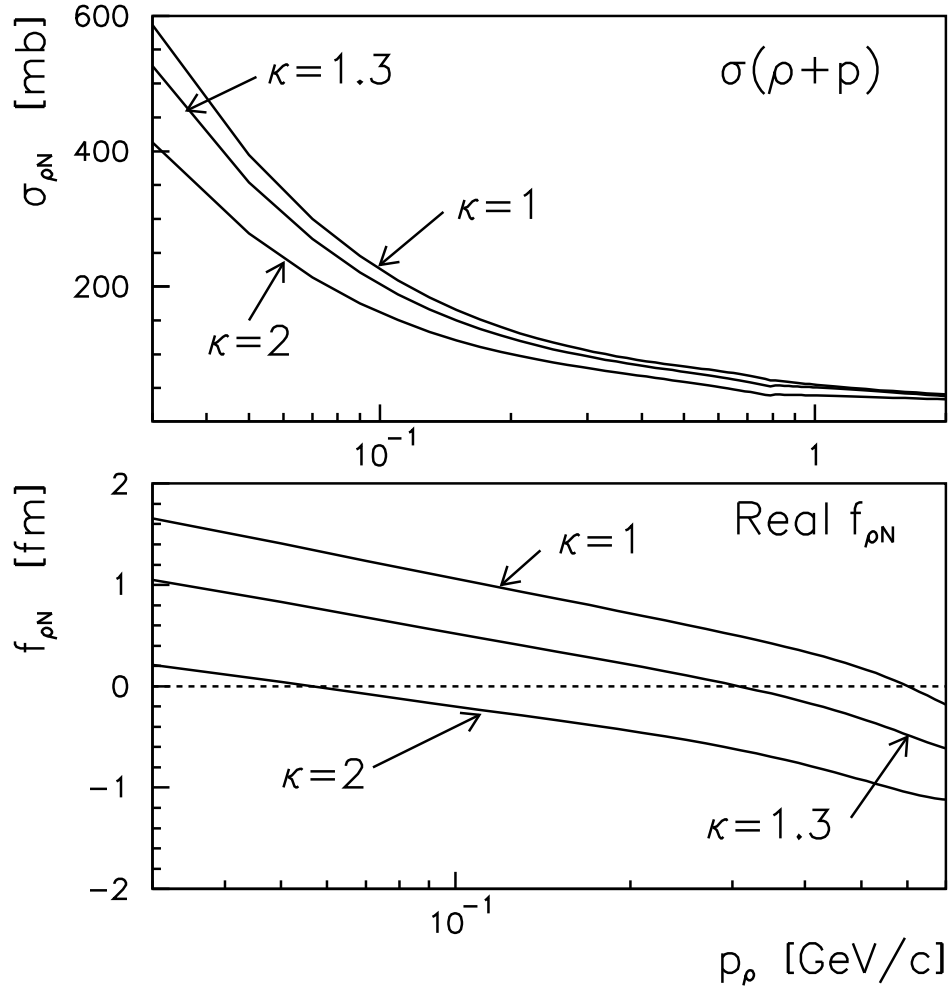


Figure 11: The total ρN cross section and the real part of the ρN scattering amplitude calculated with different widths of the baryonic resonances. The factor κ indicates the ratio of the in-medium resonance width to its vacuum width.